Chinese Journal of Structural Chemistry xxx (xxxx) xxx

Contents lists available at ScienceDirect

Chinese Journal of Structural Chemistry

journal homepage: www.journals.elsevier.com/chinese-journal-of-structural-chemistry

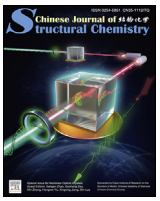

Short Communication

Confined proton transport in water-containing layered manganese oxide electrodes

Wenwei Cai, Feng Pan *, Shunning Li **

School of Advanced Materials, Peking University, Shenzhen Graduate School, Shenzhen, 518055, China

Understanding the proton dynamic behavior in inorganic materials has long been a topic of intense fascination [1], especially in the field of electrochemical energy storage [2]. One of the examples is the research of proton transport in transition metal oxides, which dates back to 1971 [3] when RuO_2 was discovered to be capable of storing protons via reversible redox reactions [4]. In aqueous electrolytes, the thin film RuO_2 electrode exhibits a surface pseudocapacitive behavior [5], which could be modified by the structural water in its hydrated form due to the facile Grotthuss hopping mode of protons along the established hydrogen bonds inside the bulk phase [6]. Soon later, Goodenough et al. reported the capacitor-like behavior of amorphous $MnO_2{\cdot}xH_2O$ electrode in an aqueous KCl electrolyte [7], and further studies on the hydrated MnO_2 electrodes prepared by sol-gel processes have soon discovered that the intercalation of protons from aqueous electrolytes plays an indispensable role in the charge storage mechanism [8]. In recent years, the research interest on rechargeable aqueous batteries has fueled the renaissance of mechanistic study of proton transport in transition metal oxides [9], which can operate as cathodes or anodes via a topotactic insertion mechanism similar to that in Li-ion batteries [10]. However, due to the challenges for experimental detection of local chemical environments of the inserted protons, a comprehensive understanding of proton dynamic behavior in these electrodes remains largely lacking.

Among various cathode materials that can store proton charge carriers [11], Mn-based oxides have garnered considerable attention [12], for which previous computer simulations have found that protons situated at the vacant sites in their bulk phase can migrate in a concerted way [13,14], similar to the diffusion-free Grotthuss model in liquid water. This raises a question of how the inclusion of water molecules inside the metal oxide frameworks modulates the proton motion. Several studies have indicated that confined water in tunnel/layered architectures of oxide materials could form hydrogen bond chains or networks with a collective reorientation effect imposed by metal cations and oxygen anions [15]. It is therefore crucial to evaluate how this effect regulates the proton dynamic behavior in Mn-based oxide electrodes, which is linked to the (de)intercalation of protons and consequently the electrochemical performance in terms of reversible capacity, rate capability and cycle life.

In this work, layered-phase δ-MnO_2 is employed as a prototypical example to study the rich transitional dynamics related to proton transport in the interlayer space filled with water. Our results show that the proton transport efficiency can be significantly influenced by the interlayer distance and the proton concentration, both of which could alter the adsorption state of protons on MnO_2 and the ordering of interfacial water molecules, leading to a confinement-induced proton trapping effect.

Fig. 1(a) shows a snapshot of the atomic configuration with an interlayer distance of 11 Å and a proton concentration of 8 additional H atoms per supercell in the *ab initio* molecular dynamics (AIMD) simulations. It is noted that most of the additional H atoms will be adsorbed at the surface of the MnO_2 slab, while the remaining ones will reside in the aqueous phase, producing H_3O^+. The H adsorbates (H_{ads}) directly form O−H bonds of around 1.0 Å with the lattice oxygen atoms of MnO_2, close to the O−H bond lengths in water molecules, which indicates the similarity in bond strength for both cases. Hydrogen bonds are also dominant between H atoms in the interfacial H_2O/H_3O^+ molecules and O atoms in MnO_2, giving rise to the first peak in the density distribution profile of H atoms in the aqueous phase (denoted as H_{aq}). The O atoms in the interfacial H_2O/H_3O^+ are distributed at around 2.6 Å from the O layer in MnO_2, and this value hardly varies with different interlayer distances and proton concentrations (Fig. S1).

To investigate the proton transport events between the MnO_2 slab and aqueous phase, we can rely on the free energy profile for each configuration, as derived from the probability density of proton transport coordinates during the transition from an adsorption state (H_{ads}) to a hydrated state (H_3O^+) in the interfacial water layer. Fig. 1(b–c) shows that the saddle point in the free energy surface (see Methods in SI) for proton hopping lies near the middle point between the lattice O at the MnO_2 slab and the O atom of water molecule in the aqueous phase. The distance between both O atoms will shrink to 2.35−2.45 Å when the proton crosses the saddle point. The symmetry in these energy profiles suggests that there

* Corresponding author.
** Corresponding author.
E-mail addresses: panfeng@pkusz.edu.cn (F. Pan), lisn@pku.edu.cn (S. Li).

https://doi.org/10.1016/j.cjsc.2025.100528
Received 5 December 2024; Received in revised form 17 January 2025; Accepted 19 January 2025
0254-5861/© 2025 Fujian Institute of Research on the Structure of Matter, Chinese Academy of Sciences. Published by Elsevier B.V. All rights are reserved, including those for text and data mining, AI training, and similar technologies.

Please cite this article as: W. Cai et al., Confined proton transport in water-containing layered manganese oxide electrodes, Chinese Journal of Structural Chemistry, https://doi.org/10.1016/j.cjsc.2025.100528

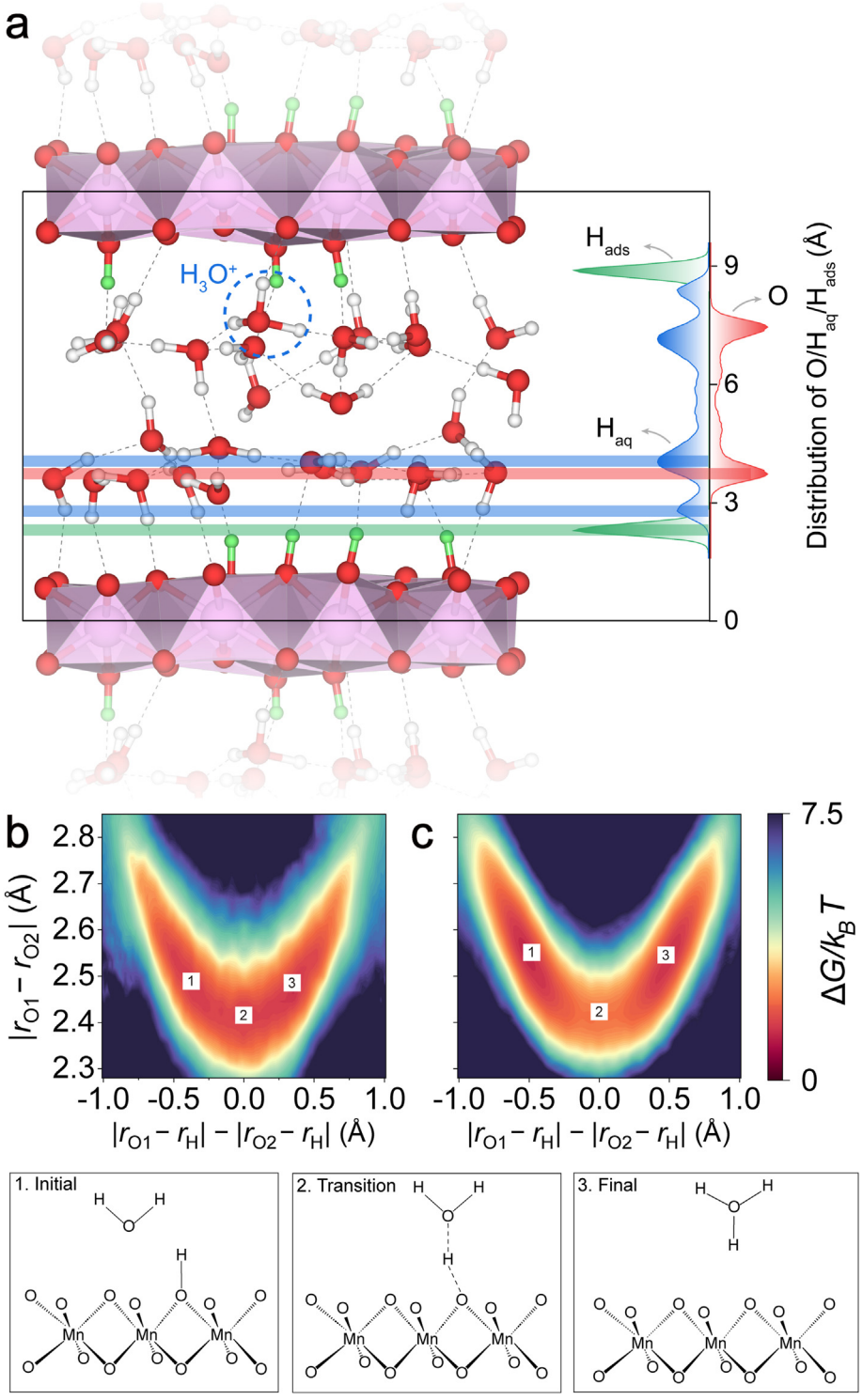

Fig. 1. δ-MnO_2 with water molecules and additional H atoms distributed in the interlayer space, and the explicative free energy surfaces for proton transport. (a) A snapshot of the AIMD simulations. The plots on the right show the corresponding density distribution profiles of O atoms in H_2O/H_3O^+, H atoms in H_2O/H_3O^+ (H_{aq}) and H adsorbates on δ-MnO_2 (H_{ads}). Color code: Mn, light purple; O, red; H_{aq}, white; H_{ads}, green. (b, c) The contours of free energy surfaces for configurations at an interlayer distance of 7 Å and with (b) 1 and (c) 8 inserted H atoms per supercell, respectively. By introducing two collective variables, $|r_{O1} - r_{O2}|$ and $|r_{O1} - r_H| - |r_{O2} - r_H|$, these contours could illustrate the probability distributions of various configurations during proton transfer from the MnO_2 slab to the aqueous phase. The left basin corresponds to the state with a proton bonded to MnO_2, while the right basin corresponds to the state after forming a hydronium. The color bar illustrates the free energy in the unit of k_BT.

is hardly a bias between the undissociated state with the proton bonded to MnO_2 and the solvated state, where the proton is transferred to a closest water molecule, finally forming a hydronium and free to diffuse in the aqueous phase. Moreover, the two basins in the free energy surface plot tend to become more distant from each other with more protons in the structure (Fig. S2), which corresponds to considerably increased difficulty

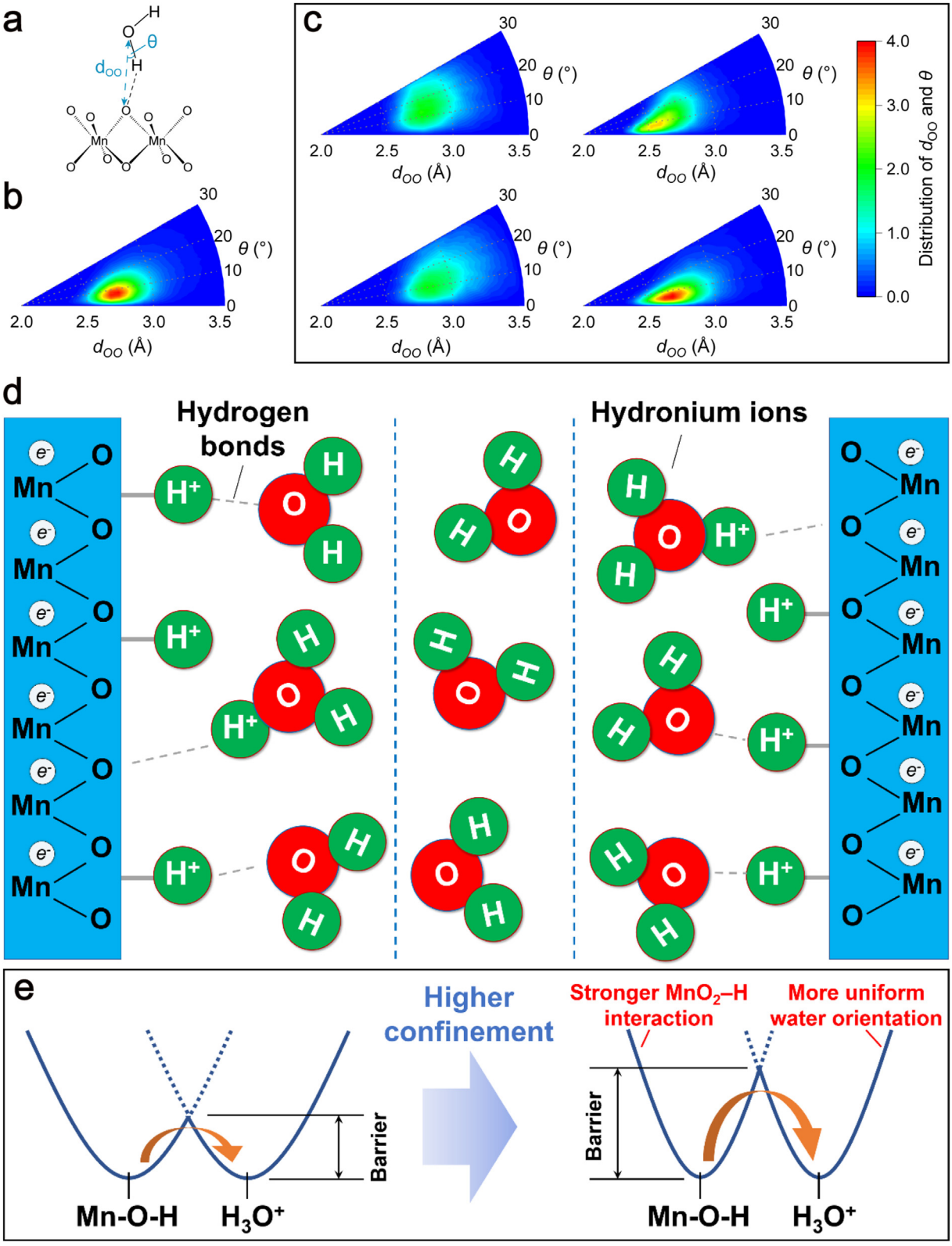

Fig. 2. Hydrogen bonds established above the MnO_2 slab and schematic illustration of confinement-induced proton trapping effect. (a) Schematic diagram of a hydrogen bond between the O atom at MnO_2 and the interfacial water molecule. (b) Distribution of d_{OO} and θ for water. (c) Distribution of d_{OO} and θ for hydrogen bonds between MnO_2 slab and the aqueous phase. The upper and lower panels correspond to interlayer distances of 7 and 15 Å, respectively, while the left and right panels correspond to proton concentration of 1 and 8 atoms/supercell, respectively. (d) The local chemical environment of protons inserted into a water-containing layered manganese oxide electrode. (e) The influence of confinement effect on the free energy landscape during the transfer of protons in the interlayer region.

for proton transfer. This result can be further substantiated by the time needed for a proton transport event in average during the simulations (Fig. S3 and Table S1), where a drastic increase in the interval for proton transport is demonstrated at high proton concentrations.

The above results indicate that the local environments of hydrogen bonds will differ significantly according to the proton concentrations. To further illustrate this, we can rely on the distribution of probability for different hydrogen bond structures, which can be described via the O•••O distance (d_{OO}) and H−O···O angle (θ), as shown in Fig. 2(a). For free water, the value of d_{OO} is primarily distributed at 2.6–2.8 Å while that of θ is around 10° (Fig. 2(b)). Fig. 2(c) and Fig. S5 show the evolution of distribution profile when the interlayer distance increases from 7 to 15 Å and the proton concentration increases from 1 to 8 atoms/supercell. Notably, the configurations at larger interlayer distance and higher proton concentration will correspond to (d_{OO}, θ) values that are more similar to those of free water. Especially, the results of low proton concentration cases are generally related with longer hydrogen bond and larger H−O•••O angle, which can be ascribed to a less strong affinity of protons to the MnO_2 slab at limited proton concentration. Moreover, for structures that exhibit identical interlayer distance, the number of hydrogen bonds related to O atoms in the MnO_2 slab will increase along with proton concentration, whereas the change in the number of hydrogen bonds in water is negligible (Fig. S6). The analysis on the orientation of water molecules in the interlayer region of δ-MnO_2 (Fig. S7) further reveals that a smaller interlayer distance and a higher proton content could give rise to higher ordering of the interfacial water. This ordering could disrupt the connectivity of hydrogen bonds and therefore give rise to sluggish kinetics of proton hopping, which is in good agreement with the larger energy barrier for proton hopping at higher proton concentrations (Fig. S2).

Accordingly, a model of confinement-induced proton trapping effect is proposed, as shown in Fig. 2(d–e). Protons can be accommodated in two states, the adsorption state with a local configuration of Mn–O–H and the hydrated state characteristic of a H_3O^+. In the former case, the positively charged protons have a strong electronic interaction with the negatively charged MnO_2 slab. Higher proton concentration will enhance this interaction, leading to a steeper energy gradient for protons that are about to detach (Fig. 2(e)). In the case of H_3O^+ configuration, the electric field of Mn–O–H gives rise to an ordered alignment of the interfacial water molecules. Shorter interlayer distance between MnO_2 slabs will result in a less dominant role of this ordering, because the opposite electric fields induced by neighboring MnO_2 slabs could interfere the orientation of water molecules in the middle of interlayer region. Higher proton concentration will imply larger electric field intensity, and thus help the orientation of water molecules. Since the O atoms on MnO_2 are at well-defined positions in the crystal structure, this orientation effect could benefit the establishment of hydrogen bonds, as evidenced by the higher similarity of both d_{OO} and θ between the highly oriented water molecules and the free water counterparts (Fig. 2(b–c)). Therefore, the more uniform water orientation configuration will finally increase the slope of the free energy surface curve for H_3O^+. The combination of rougher energy landscapes on both the Mn–O–H and H_3O^+ sides leads to the larger kinetic barrier for proton migration, which will inevitably influence the proton storage process in δ-MnO_2 electrode.

In conclusion, we have deciphered the atomic structures of confined water in layered-phase δ-MnO_2 and the corresponding proton dynamic behavior. The interlayer distance between MnO_2 slabs and the concentration of protons in the interlayer space are demonstrated to be critical factors dictating the local chemical environments of hydrogen bonds. The insights in this work will deepen our understanding of confined proton transport and facilitate the design of proton storage electrodes with high capacity and rate capability in the field of rechargeable aqueous batteries.

CRediT authorship contribution statement

Wenwei Cai: Writing – original draft, Formal analysis, Data curation. **Feng Pan:** Writing – review & editing, Supervision, Funding acquisition, Formal analysis. **Shunning Li:** Writing – review & editing, Funding acquisition, Formal analysis, Conceptualization.

Declaration of competing interest

The authors declare no competing interests.

Acknowledgements

The authors acknowledge financial support from the National Natural Science Foundation of China (22109003), the Basic and Applied Basic Research Foundation of Guangdong Province (2023A1515011391), Soft Science Research Project of Guangdong Province (No. 2017B030301013), and the Major Science and Technology Infrastructure Project of Material Genome Big-science Facilities Platform supported by Municipal Development and Reform Commission of Shenzhen.

Appendix A. Supplementary data

Supplementary data to this article can be found online at https://doi.org/10.1016/j.cjsc.2025.100528.

References

[1] L. Vilciauskas, M.E. Tuckerman, G. Bester, S.J. Paddison, K.D. Kreuer, The mechanism of proton conduction in phosphoric acid, Nat. Chem. 4 (2012) 461–466.
[2] L.T. Zhang, C. Zhang, E.J. Berg, Mastering proton activities in aqueous batteries, Adv. Mater. (2024) 2407852.
[3] S. Trasatti, G. Buzzanca, Ruthenium dioxide: a new interesting electrode material. Solid state structure and electrochemical behaviour, J. Electroanal. Chem. Interfacial Electrochem. 29 (1971) A1–A5.
[4] S. Ardizzone, G. Fregonara, S. Trasatti, "Inner" and "outer" active surface of RuO_2 electrodes, Electrochim. Acta 35 (1990) 263–267.
[5] V. Augustyn, P. Simon, B. Dunn, Pseudocapacitive oxide materials for high-rate electrochemical energy storage, Energy Environ. Sci. 7 (2014) 1597–1614.
[6] W. Sugimoto, H. Iwata, K. Yokoshima, Y. Murakami, Y. Takasu, Proton and electron conductivity in hydrous ruthenium oxides evaluated by electrochemical impedance spectroscopy: the origin of large capacitance, J. Phys. Chem. B 109 (2005) 7330–7338.
[7] H.Y. Lee, J.B. Goodenough, Supercapacitor behavior with kcl electrolyte, J. Solid State Chem. 144 (1999) 220–223.
[8] S.C. Pang, M.A. Anderson, T.W. Chapman, Novel electrode materials for thin-film ultracapacitors: Comparison of electrochemical properties of sol-gel-derived and electrodeposited manganese dioxide, J. Electrochem. Soc. 147 (2000) 444.
[9] D. Chao, W. Zhou, F. Xie, C. Ye, H. Li, M. Jaroniec, S.-Z. Qiao, Roadmap for advanced aqueous batteries: from design of materials to applications, Sci. Adv. 6 (2020) eaba4098.
[10] M. Li, X. Wang, J. Meng, C. Zuo, B. Wu, C. Li, W. Sun, L. Mai, Comprehensive understandings of hydrogen bond chemistry in aqueous batteries, Adv. Mater. 36 (2024) 2308628.
[11] S. Wu, H. Guo, C. Zhao, Challenges and opportunities for proton batteries: from electrodes, electrolytes to full-cell applications, Adv. Funct. Mater. 34 (2024) 2405401.
[12] X. Jia, C. Liu, Z.G. Neale, J. Yang, G. Cao, Active materials for aqueous zinc ion batteries: synthesis, crystal structure, morphology, and electrochemistry, Chem. Rev. 120 (2020) 7795–7866.
[13] R. Qin, S. Ding, C. Hou, L. Liu, Y. Wang, W. Zhao, L. Yao, Y. Shao, R. Zou, Q. Zhao, S. Li, F. Pan, Modulating the proton-conducting lanes in spinel $ZnMn_2O_4$ through off-stoichiometry, Adv. Energy Mater. 13 (2023) 2203915.
[14] Q. Zhao, A. Song, W. Zhao, R. Qin, S. Ding, X. Chen, Y. Song, L. Yang, H. Lin, S. Li, F. Pan, Boosting the energy density of aqueous batteries via facile grotthuss proton transport, Angew. Chem. Int. Ed. 60 (2021) 4169–4174.
[15] T. Xu, Z. Xu, T. Yao, M. Zhang, D. Chen, X. Zhang, L. Shen, Discovery of fast and stable proton storage in bulk hexagonal molybdenum oxide, Nat. Commun. 14 (2023) 8360.